JOURNAL OF MATERIALS SCIENCE 19 (1984) 2195–2202

Fracture of translucent alumina: temperature dependence and influence of CaO dope

G. DE WITH
Philips Research Laboratory, P.O. Box 80 000, 5600 JA, Eindhoven, The Netherlands

The influence of CaO on the mechanical behaviour of translucent, MgO-doped Al_2O_3 ceramics has been investigated, using alumina both without and with added CaO. The addition of only 40 wt ppm CaO drastically changed the microstructure, resulting in an increase of optical transmission, which was the purpose of the addition. Strength (~300 MPa) and fracture toughness (~3.7 MPa $m^{1/2}$), however, as measured at room temperature, decreased by 30% and 10%, respectively, while the resistance to slow crack growth increased slightly. Toughness as well as strength, showed a relative decrease with temperature of about 3×10^{-4} K^{-1}. The results are discussed and compared with available literature data.

1. Introduction

The influence of CaO addition on the properties of MgO-doped translucent alumina ceramic has not been investigated in detail. This addition is of interest since it increases the optical transmission of the ceramic. Fears that the CaO dope might degrade the mechanical properties of the material because it segregates heavily at the grain boundaries, seem to be confirmed by experiments on (opaque) debased alumina, which indeed indicate a decreasing fracture toughness and strength with increasing CaO content at the fracture surface [1, 2, 31]. However, the fracture toughness of hot-pressed alumina containing no MgO was found to be independent of the CaO content [3]. Therefore, some experiments were started with a view to obtaining more information on the mechanical properties of CaO-doped translucent alumina.

2. Experimental procedure

The materials were prepared using a commercially available starting powder*, disagglomerated by the manufacturer. X-ray diffraction revealed that this powder contained about 95% α-Al_2O_3 and 5% γ-Al_2O_3. The specific surface area, A, as measured with standard N_2-BET technique, amounts to about 15 m^2 g^{-1}. The corresponding mean primary particle diameter, d, as calculated from $d = 6/\rho_{th}A$, where ρ_{th} is the X-ray density, was 0.10 μm. The main impurities, determined by spectrochemical analysis, were (wt ppm in brackets): Na (24), K (60), Fe (30), Ga (30) and Si (40).

Sinter powder was prepared by addition of 100 wt ppm MgO. To one batch 40 wt ppm CaO was also added. The required amounts of additions were added as a solution of the ethanoic salts in ethanol.

Resulting powders were viewed under a scanning electron microscope (SEM) to obtain a general view of the powder. Agglomerates containing many primary particles were observed. A semi-quantitative estimate of the mean agglomerate diameter was made by the centrifuge technique, resulting in about 0.6 μm.

After sieving through a 100 μm diameter mesh, the powders were pre-pressed in a perspex die at about 5 MPa. Typical dimensions of the resulting blocks were 3 cm x 3 cm x 8 cm. Each compact was then vacuum-sealed in plastic bags and isostatically pressed at 100 MPa.

The blocks were prefired at 1100 K in oxygen for 2 h using a heating and cooling rate of 60 K h^{-1}. Sintering was carried out in a vacuum of

*Ugine Kuhlman, A15Z.

0022–2461/84 $03.00 + .12

approximately 10^{-5} torr*. The sintering programme was as follows: an initial heating rate of 150 K h^{-1} to 1800 K, this level was held for 1 h, the same heating rate was then re-applied to 2150 K, this temperature was maintained for 8 h, followed by a cooling rate of 100 K h^{-1} back to room temperature. The intermediate level in the sintering scheme was applied in order to avoid the inclusion of residual pores within the grains.

The microstructure of the materials was revealed, after polishing down to 2 μm diamond paste, by thermal etching at 1900 K for 3 h at a vacuum of about 10^{-5} torr. Micrographs of the two materials, from now on referred to as the Al_2O_3(MgO) and Al_2O_3(MgO, CaO) ceramic, were used to determine the intercept distributions of the grains with the aid of a digital planimeter†. Approximately 1500 grains were counted for each material.

The density, ρ, of the two materials was determined using the method described by Prokic [4]. The longitudinal wave velocity, v_l, and the shear wave velocity, v_s, were determined at 10 and 20 MHz, respectively, using the pulse-echo technique‡ [5]. Young's modulus, E, and Poisson's ratio, ν, were calculated from ρ, v_l, and v_s using the conventional formulae for isotropic materials [5]. No correction was made for attenuation since the loss tangent was less than 0.03.

The amount of dope in the resulting ceramics was determined by wet chemical analysis. From both materials specimens of size 1 mm x 3 mm x 5 mm were sawn using a diamond wheel containing 300 mesh (~54 μm) diamond grains. Strength, σ_f, and fracture toughness, K_{IC}, were measured at various temperatures using an all ceramic three-point bending set-up (span 12 mm) and a platinum-resistance furnace. For the fracture toughness, K_{IC}, this small type of specimen makes an efficient use of the material available, meanwhile retaining accuracy and reliability [6]. The specimens were kept for 15 min at the test temperature before fracturing. All measurements were carried out in a dry flowing nitrogen atmosphere (20 litre min^{-1}, ~200 ppmV H_2O, corresponding to ~0.7% r.h.) to minimize slow crack growth. In all cases the crosshead speed of the testing machine§ was 0.1 mm min^{-1}, corresponding to a strain rate of 2.1×10^{-4} sec^{-1} [7]. For both the σ_f and the K_{IC} measurement at each temperature five specimens were used. The fracture toughness specimens were notched with a width ~100 μm and relative depth ~0.15. Pre-cracking was done by means of a Knoop or Vickers hardness indentation (1 or 2 N load) just below the notch tip on both sides of the specimen. The value of the compliance factor was calculated according to Brown and Srawley [8].

Scanning electron micrographs (SEM) were taken from a fracture surface of a specimen fractured at each temperature. The fracture surface was covered with a thin gold layer to avoid charging effects.

The slow crack growth behaviour was determined by the strain-rate technique [9] using strain rates of 2.1×10^{-5}, 2.1×10^{-4} and 2.1×10^{-3} sec^{-1}. Here at each strain rate nine specimens were measured in a controlled wet nitrogen atmosphere (~75% r.h.). The strength–strain rate data were analysed using both the median value and the homologue series methods [9].

Finally, in order to check the supposed increase in optical transmission, the total and in-line transmission, T_T and T_D, respectively, were measured over the wavelength range 200 to 2500 nm using 500 μm thick polished plates. The spectrometer used was equipped with an integrating sphere to measure T_T. For T_D, only light scattered in a half-angle of 5° was collected.

3. Results and discussion

This section deals successively with the material characteristics, room temperature values of the mechanical properties, the influence of the CaO dope on these properties and their temperature dependence.

3.1. Material characteristics

The material characteristics are presented in Table I. It is clear from this table that about 8% MgO was lost during sintering, whereas no CaO was lost. The density is nearly equal to the theoretical value. As can be seen from Fig. 1, the grain-size distribution of the Al_2O_3(MgO) ceramic seems fairly regular, while that of the Al_2O_3(MgO, CaO) material looks somewhat more irregular. However,

*Astro 1100 V.
†MOP-Kontron-AM-03.
‡Panametrics 5223.
§Overload Dynamics S200.

TABLE I Material characteristics*

Material	Al_2O_3(MgO)	Al_2O_3(MgO, CaO)
MgO (wt ppm)	92 (5)	92 (5)
CaO (wt ppm)	2 (1)	41 (3)
ρ (g cm^{-3})	3.984 (0.002)	3.983 (0.002)
ρ (%)†	99.94	99.92
D_{50} (μm)	23	36
S (= ln D_{50}/D_{16})	0.7	1.0
E (GPa)	406 (2)	397 (2)
ν	0.241 (0.002)	0.243 (0.002)
T_T (%)‡	72.5	77.5
T_D (%)‡	39.5	54.5

*For symbols used see text, sample standard deviation given in parentheses.
†Assuming the theoretical density ρ_{th} = 3.986 g cm^{-3}.
‡Measured at λ = 600 nm for 500 μm thick specimens polished on both sides.

from the intercept distribution measurements it is clear that neither of the two materials has a pure log-normal distribution (Fig. 2). Hence only the mode, D_{50}, and overall standard deviations, S, are presented in Table I.

The value for E = 406 GPa is in good agreement with the value of 404 GPa, determined by Chung and Simmons [10]. It is also in good agreement with the value calculated for Young's modulus of polycrystalline material from the single-crystal elastic constants according to the Voigt–Reuss–Hill averaging scheme [11].

Addition of CaO indeed has the effect of increasing the optical transmission, in-line as well as total, over the whole wavelength range measured. For the more important of the two, total transmission, this increase is 5% at 600 nm. As stated in Section 1, this was the main reason for doping with CaO. Since the densities of the two materials are nearly the same, this increase is entirely due to the differences in microstructure.

3.2. Room temperature data

The values for K_{IC} and σ_f at room temperature are 3.7 MPa m$^{1/2}$ and 298 MPa, respectively (Table II). A comparison of the K_{IC} and σ_f data for translucent aluminas as published in the literature

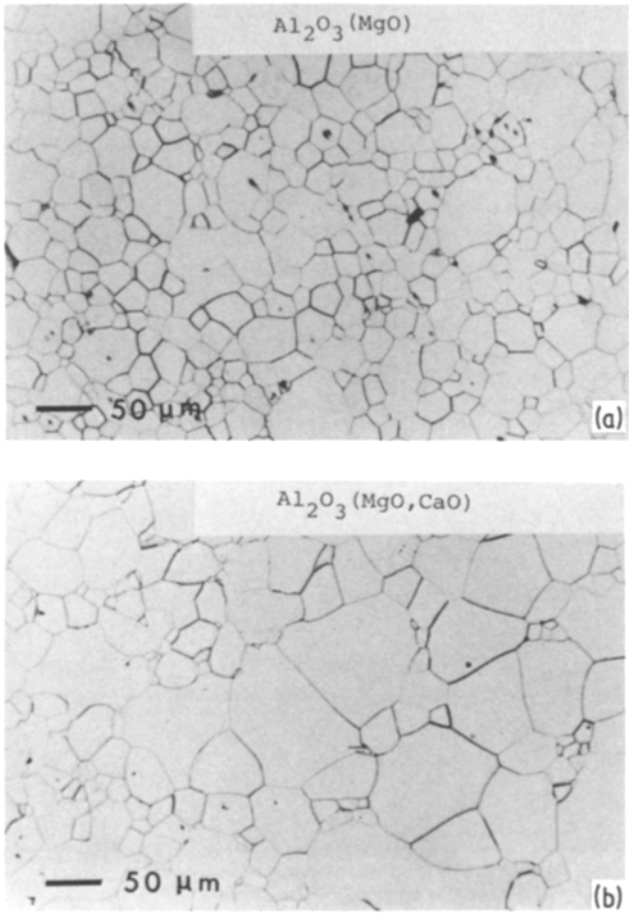

Figure 1 Microstructure of (a) the Al_2O_3 (MgO) ceramic and (b) the Al_2O_3(MgO, CaO) ceramic.

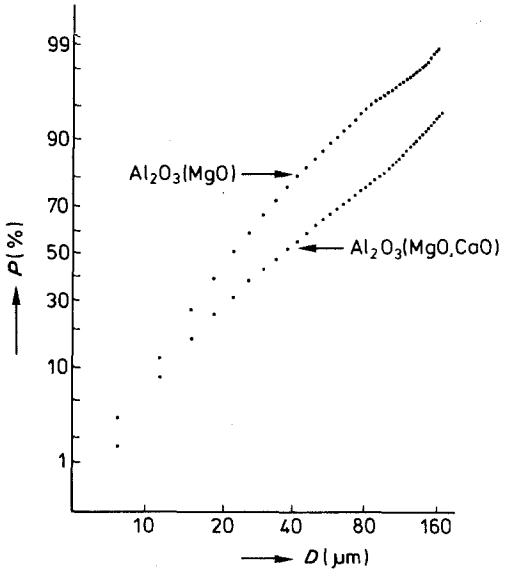

Figure 2 Log-normal plot of the intercept distributions.

is given in Table III. For K_{IC} two trends are visible. Firstly, an increase of K_{IC} with D when measured with the double cantilever beam technique. Secondly, a more or less D-independent value for K_{IC} when measured with the bend technique. This controversy has been observed for a number of materials and is discussed at length in the literature (see e.g. [20]). In most of these investigations, a K_{IC} value somewhere around 4 MPa m$^{1/2}$ is quoted. Our value, 3.7 MPa m$^{1/2}$, fits nicely in the range of observed values, although perhaps a little on the low side. Finally, there is the somewhat high value of 4.9 MPa m$^{1/2}$ as determined by Evans [17, no. 8 in Table II] using the double torsion technique.

TABLE II Mechanical properties at room temperature*

Material	Al_2O_3(MgO)	Al_2O_3(MgO, CaO)
K_{IC} (MPa m$^{1/2}$)	3.71 (0.25)	3.28 (0.72)
σ_f (MPa) as-sawn	298 (39)	204 (24)
σ_f (MPa) annealed (1700 K, 1 h, 10^{-5} torr)	280 (28)	161 (23)
n	36	44
A (m sec^{-1})	63	86
r† (%)	99	90

*For symbols used see text, sample standard deviation given in parentheses.
†Regression coefficient for median value analysis.

There is no clear explanation for this result.

The strength, σ_f, decreases with increasing grain size, D, ranging from $\sigma_f \sim 340$ MPa at $D \sim 10\,\mu$m to $\sigma_f \sim 240$ MPa at $D \sim 30\,\mu$m. Our data belong to the middle of the range: $\sigma_f \sim 298$ MPa at $D \sim 23\,\mu$m.

Since a residual stress, σ_r, may be present as a result of the machining operation, an annealing treatment of 1 h at 1700 K was applied, reducing the strength from 298 to 280 MPa (Table II). The surface morphology of the as-sawn and annealed specimens, observed by means of the SEM technique, showed no significant differences. Because the original strength was 298 MPa, a residual compressive stress of about 20 MPa was present.

An estimate of the mean critical flaw size, a_c, can be made from the equation

$$K_{IC} = Y(\sigma_f + \sigma_r)a_c^{1/2} \quad (1)$$

TABLE III Comparison of mechanical properties of translucent aluminas at room temperature

No.	K_{IC} (MPa m$^{1/2}$)	Method*	σ_f (MPa)	Method*	D (μm)	Fracture mode	Reference
1	4.7†	3-pb	–	–	22	mainly intergranular	[12]
2	3.96	3-pb	–	–	25	entirely intergranular	[13]
3	4.1	DT, DCB	275	flexural	35	almost completely intergranular	[14]
4	3.7	DT, DCB	345	flexural	8		[14]
5	4.0†	3-pb	–	–	35	intergranular?	[15]
6	5.1	DCB	–	–	35		[15]
7	4.41	short bar	–	–	20	–	[16]
8	4.9	DT	230	4-pb	30	–	[17]
9	–	–	348	3-pb	5–10	preferably intercrystalline	[18]
10	–	–	280	3-pb	20–25		[18]
11	–	–	240	3-pb	30–35		[18]
12	3.8	DCB	–	–	10	mixed	[19]
13	4.8	DCB	–	–	30		[19]
14	6.1	DCB	–	–	45		[19]
15	3.71	3-pb	278	3-pb	23		this work

*3(4)-pb = three (four)-point bend, DT = double torsion, DCB = double cantilever beam.
†Calculated from the quoted γ-values using $K_{IC} = (2\gamma E)^{1/2}$ assuming $E = 400$ GPa.

assuming $Y \sim 1.26$, a value appropriate for semi-circular surface flaws [21]. Using the strength after the annealing treatment (and thus $\sigma_r = 0$), calculation of a_c results in 110 μm. This is about twice the average diamond grain size in the sawing wheel used, or five times the average intercept length D_{50}.

Subcritical crack growth is often described by the semi-empirical relation

$$\dot{a} = A(K_I/K_{IC})^n \quad (2)$$

where $\dot{a}$ is the crack growth rate and K_I the applied stress intensity factor. For the Al_2O_3(MgO) ceramic a value of 36 (Table II), was determined, from strain-rate experiments [9]. Fairly similar results were obtained from the median value and homologue series analysis. Only one other determination of n could be located in the literature [18]. In that experiment the double torsion technique was used, resulting in $n = 52$ for translucent alumina with an average grain size of 30 μm as tested in water. Part of the difference may be due to differences in crack geometry, natural microcracks being studied in the strain-rate experiments and an induced macrocrack in the double torsion experiment. Further differences between the two materials are D_{50} and possibly purity, while the difference in testing conditions ($\sim$ 75% r.h. compared with water) may also result in different values for n.

3.3. The influence of CaO

It is well known that calcium segregates heavily on grain boundaries of alumina [2, 29, 30]. Although there is no conclusive evidence, the presence of CaO at the grain boundaries possibly leads to the formation of $CaO \cdot 6Al_2O_3$. Since this compound has a layered structure, the grain-boundary phase is expected to be weaker than the bulk phase. A negative influence on the mechanical properties is thus expected. This has indeed been observed for K_{IC} [1, 2] as well as σ_f [31] in the case of debased alumina.

Upon the addition of CaO in translucent alumina, a slight decrease in K_{IC} ($\sim$ 10%) as well as a substantial decrease in σ_f ($\sim$ 30%) is observed (Table II).

A similar decrease in K_{IC} (10 to 20%) was also observed for debased alumina [1, 2] containing about the same amount of CaO. This behaviour is contrary to that of hot-pressed alumina with CaO dope, where no decrease in K_{IC} was observed [3]. Aside from the difference in grain size (which is not essential for the bend technique used as discussed earlier) and the absence of MgO in the hot-pressed material (which in our material is probably dissolved entirely in the lattice [23]), an essential difference is the fracture mode. The fracture mode of the hot-pressed material was mainly transgranular. Since the CaO is heavily segregated at the grain boundaries [2, 29, 30] this addition is expected to have little influence in the case of transgranular fracture. On the other hand, for intergranular fracture a significant influence is expected.

The decrease of σ_f ($\sim$ 30%) cannot be entirely explained by the decrease in K_{IC} ($\sim$ 10%). The influence of residual surface stress, as well as the difference in average grain size, has to be considered. The influence of the surface stress in the Al_2O_3(MgO, CaO) ceramic was estimated similarly to that for the Al_2O_3(MgO) material, and a strength decrease of $\sim$ 40 MPa was found, which is twice the value for the Al_2O_3(MgO) ceramic. In view of the larger value of D_{50} for this material a somewhat higher value for the residual stress is not unexpected. If we assume that the critical flaw is contained in one grain, an estimate of the probability of having such a flaw, P_f, can be made from Fig. 2. For the Al_2O_3(MgO) ceramic with $a_c \sim 110\,\mu$m, this leads to $P_f \sim 3\%$. Further assuming the same probability for the Al_2O_3(MgO, CaO) ceramic, extrapolation of the appropriate curve in Fig. 2 leads to $D = a_c \sim 250\,\mu$m. Using Equation 1 with the data discussed yields $\sigma_f \sim$ 210 MPa, in good agreement with the experimental value of 204 MPa.

The parameter n in Equation 2, surprisingly, increases somewhat upon CaO addition (Table II). It is not clear why. In any case, the slow crack-growth rate is not substantially increased upon CaO addition, unlike the deterioration of K_{IC} and σ_f.

The value of E for the Al_2O_3(MgO, CaO) ceramic, 397 GPa, is somewhat lower than that for the reference material, 406 GPa. Since the densities are virtually equal and no crystallographic texture was present (as verified by X-ray techniques) this lower value is attributed to a slight amount of microcracking resulting from the large grains in the grain-size distribution.

3.4. Temperature dependence

Figs. 3 and 4 show the temperature dependence of K_{IC} and σ_f. Both strength and fracture toughness

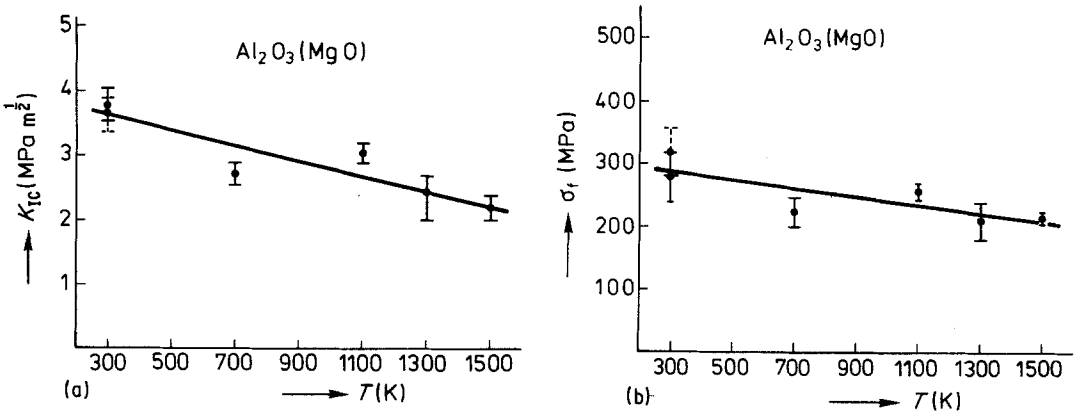

Figure 3 (a) Fracture toughness and (b) strength of the Al_2O_3(MgO) ceramic.

show a relative decrease with temperature of -2×10^{-4} to $-3 \times 10^{-4}\,K^{-1}$.

Although several investigators report the temperature dependence of K_{IC} for debased alumina, only Evans *et al.* quote quantitative results for translucent alumina [17]. Unfortunately, their room temperature result is the high value mentioned earlier. Fitting their data up to 1500 K with a linear relationship yields a value $1/K_{IC}(300\,K) \cdot dK_{IC}/dT = -3.4 \times 10^{-4}\,K^{-1}$. Our data result in almost the same value ($-3.0 \times 10^{-4}\,K^{-1}$). Excellent agreement is thus achieved for the relative decrease in fracture toughness with temperature.

With increasing temperature the fracture mode changes from "mixed" to "completely intergranular" (Figs. 5 to 7). Evans *et al.* [17] do not mention this change in fracture mode but several other authors do [18, 22]. In particular, Ohari and Parikh [18] present a rather elaborate discussion of the fracture morphology. Our observations for the Al_2O_3(MgO) ceramic are in agreement with their results. Furthermore, the differences in microstructure between the two materials, which were not particularly clear from the micrographs (Fig. 1), become rather clear from the fractographs (Figs. 5 to 7). The Al_2O_3(MgO) ceramic has a regular microstructure whereas the CaO-doped material is found to have large grains embedded in a matrix of much smaller grains. It should be kept in mind, however, that the intercept analysis (Fig. 2) showed an irregular, i.e. non-log-normal, distribution for both materials.

The temperature dependence of K_{IC} can be estimated using an elastic model (Appendix III [24]). According to this model the temperature dependence of K_{IC} is given by

$$\left(\frac{1}{K_{IC}}\right)\left(\frac{dK_{IC}}{dT}\right) = \frac{1}{E}\left(\frac{dE}{dT}\right) - \tfrac{1}{2}\alpha \qquad (2)$$

where α is the linear thermal expansion coefficient.

For alumina the temperature dependence of E has been determined by several investigations [10, 25, 26]. Good agreement is found between

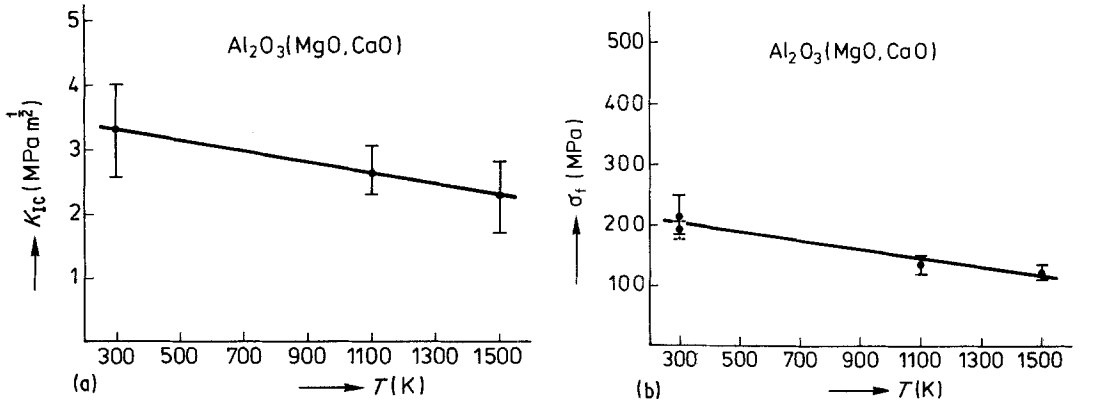

Figure 4 (a) Fracture toughness and (b) strength of the Al_2O_3(MgO, CaO) ceramic.

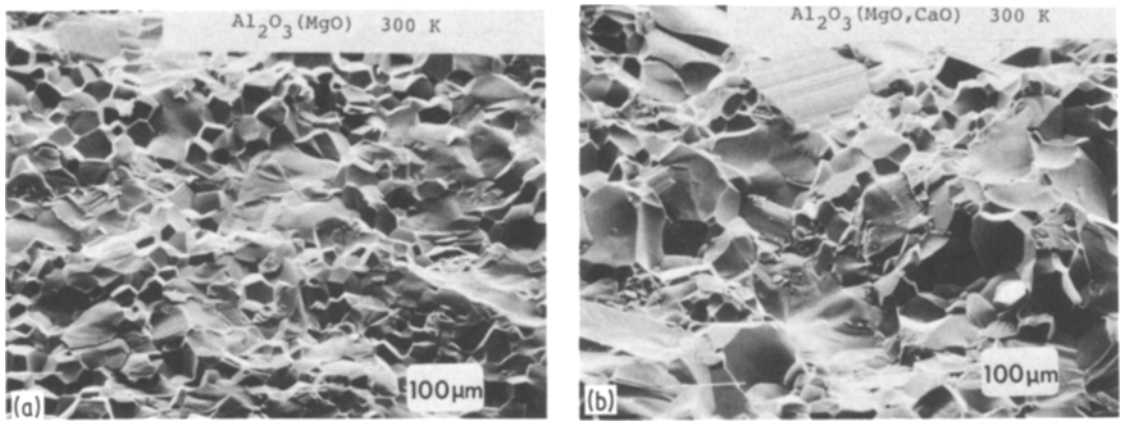

Figure 5 Fractographs of (a) the Al_2O_3(MgO) ceramic and (b) the Al_2O_3(MgO, CaO) ceramic fractured at room temperature (SEM, 45°).

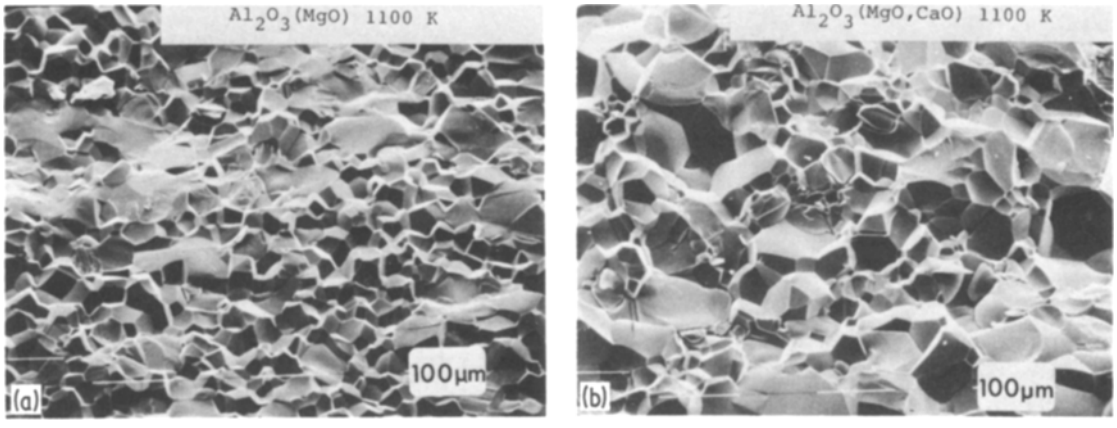

Figure 6 Fractographs of (a) the Al_2O_3(MgO) ceramic and (b) the Al_2O_3(MgO, CaO) ceramic (right) fractured at 1100 K (SEM, 45°).

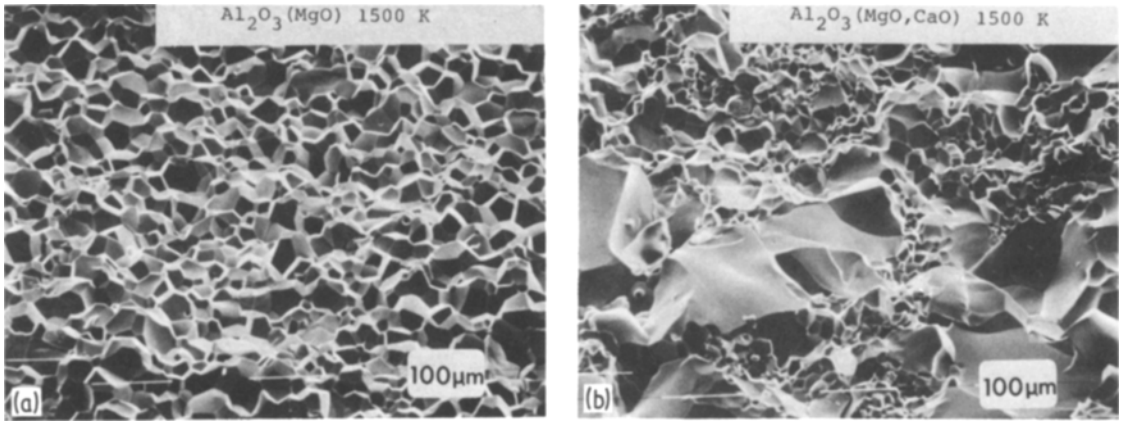

Figure 7 Fractographs of (a) the Al_2O_3(MgO) ceramic and (b) the Al_2O_3(MgO, CaO) ceramic fractured at 1500 K (SEM, 45°).

the different experiments. A linear relationship between E and T exists from 300 up to 1400 K. From the data given by Chung and Simmons [10] the temperature derivative of E is calculated to be $dE/dT = -5.4 \times 10^{-2}$ GPa K^{-1} while $E(300) = 404$ GPa. The relative change in E is thus $(1/E)(dE/dT) = -1.3 \times 10^{-4}$ K^{-1}.

The thermal expansion coefficient of alumina has also been well investigated [27, 28]. From the data given by Wachtman *et al.* [27] the overall coefficient up to 1300 K is calculated to be $\alpha = (1/\Delta T)(\Delta l/l) = 8.0 \times 10^{-6}$ K^{-1}.

The calculated value for $(1/K_{IC})(dK_{IC}/dT)$ is thus -1.3×10^{-4}. The calculated value is dominated by the changes in E with temperature and α has little influence. Comparison with the experimental value shows an order of magnitude agreement. The change in fracture mode is one possible reason for the larger decrease observed experimentally.

4. Conclusions

The influence of CaO on the fracture behaviour of translucent MgO-doped alumina has been investigated. The positive influence of CaO on the optical transmission, which is the purpose of the addition, has been confirmed. Only a minor amount of CaO drastically changed the microstructure, resulting at room temperature in a 10% and 30% decrease in fracture toughness of 3.7 MPa m$^{1/2}$ and strength of 300 MPa, respectively. The slow crack-growth behaviour at room temperature and the temperature dependence of fracture toughness and strength are rather similar for the CaO-doped and non-doped material. The main effect of CaO is thus a deterioration of the short-term mechanical characteristics: fracture toughness and strength.

Acknowledgements

Many thanks are due to N. Hattu and H. Parren for their careful experimental work.

References

1. A. W. FUNKENBUSCH and D. W. SMITH, *Met. Trans.* 6A (1975) 2259.
2. R. S. JUPP, D. F. STEIN and D. W. SMITH, *J. Mater. Sci.* 15 (1980) 96.
3. G. DE WITH and N. HATTU, *ibid.* 16 (1981) 841.
4. D. PROKIC, *J. Phys. D. Appl. Phys.* 7 (1974) 1873.
5. H. F. POLLARD, "Sound Waves in Solids" (Pion, London 1977).
6. G. DE WITH and N. HATTU, *J. Mater. Sci.* 16 (1981) 1702.
7. G. W. HOLLENBERG, G. R. TERWILLIGER and R. S. GORDON, *J. Amer. Ceram. Soc.* 54 (1971) 196.
8. W. F. BROWN and J. E. SRAWLEY, ASTM-STP-410 (American Society for Testing and Materials, Philadelphia, 1966).
9. J. E. RITTER, in "Fracture Mechanics of Ceramics", Vol. 4, edited by R. C. Bradt, D. P. H. Hasselman and F. F. Lange (Plenum Press, New York, 1978) p. 667.
10. D. M. CHUNG and S. SIMMONS, *J. Appl. Phys.* 39 (1968) 5316.
11. R. HILL, *Proc. Phys. Soc. (London)* A65 (1952) 349.
12. L. J. GRAHAM and G. A. ALERS, in "Fracture Mechanics of Ceramics", Vol. 1, edited by R. C. Bradt, D. P. H. Hasselman and F. F. Lange (Plenum Press, New York, 1974) p. 175.
13. M. J. NOONE and R. L. MEHAN, *ibid.*, Vol. 1, p. 201.
14. S. W. FRIEMAN, K. R. McKINNEY and H. C. SMITH, *ibid.*, Vol. 2, p. 659.
15. L. A. SIMPSON, *ibid.*, Vol. 2, p. 567.
16. L. M. BARKER, *ibid.*, Vol. 3, p. 483.
17. A. G. EVANS, M. LINZER and L. R. RUSSELL, *Mater. Sci. Eng.* 15 (1974) 253.
18. O. OHARI and W. M. PARIKH, in "Fracture Mechanics of Ceramics", Vol. 1, edited by R. C. Bradt, D. P. H. Hasselman and F. F. Lange (Plenum Press, New York, 1974) p. 399.
19. P. L. GUTSHALL and G. E. GROSS, *Eng. Fract. Mech.* 1 (1969) 463.
20. B. J. DALGLEISH, P. L. PRATT, R. D. RAWLINGS and A. FAKHR, *Mater. Sci. Eng.* 45 (1980) 9.
21. G. K. BANSAL, *J. Amer. Ceram. Soc.* 59 (1976) 87.
22. J. M. SAMUELS, M. R. HOOVER Jr, L. TARKAY, G. G. JOHNSON Jr, H. A. McKINSTRY and E. W. WHITE, in "Fracture Mechanics of Ceramics", Vol. 1, edited by R. C. Bradt, D. P. H. Hasselman and F. F. Lange (Plenum Press, New York, 1974) p. 421.
23. S. K. ROY and R. L. COBLE, *J. Amer. Ceram. Soc.* 51 (1960) 1.
24. G. DE WITH, *J. Mater. Sci.* 19 (1984) 457.
25. R. W. DICKSON and E. SCHREIBER, *J. Res. Nat. Bur. Stand.* 77A (1973) 391.
26. J. B. WACHTMAN Jr and D. G. LAM Jr, *J. Amer. Ceram. Soc.* 42 (1959) 254.
27. J. B. WACHTMAN Jr, J. G. SCUDERI and G. W. CLERK, *ibid.* 45 (1962) 319.
28. Y. S. TOULOUKIAN (ed.), "Thermo Physical Properties of Matter" Vol. 13 (IFI/Plenum, New York, 1977).
29. H. C. MARCUS, J. M. HARRIS and F. J. SZALKOWSKI, in "Fracture Mechanics of Ceramics", Vol. 1, edited by R. C. Bradt, D. P. H. Hasselman and F. F. Lange (Plenum Press, New York, 1974) p. 387.
30. P. E. C. FRANKEN and A. P. GEHRING, *J. Mater. Sci.* 16 (1981) 384.
31. S. SINHAROY, L. L. LEVENSON and D. E. RAY, *Amer. Ceram. Soc. Bull.* 58 (1979) 464.

Received 19 September
and accepted 29 September 1983